Available online at www.sciencedirect.com

ScienceDirect

journal homepage: www.elsevier.com/locate/he

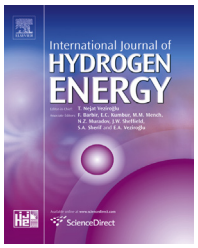

An analytical relationship for calculating the effective diffusivity of micro-porous layers

Mehdi Andisheh-Tadbir [a,b], *Mohamed El Hannach* [b], *Erik Kjeang* [b], *Majid Bahrami* [a,*]

[a] *Laboratory for Alternative Energy Conversion (LAEC), School of Mechatronic Systems Engineering, Simon Fraser University, 250-13450 102 Avenue, Surrey, BC, V3T 0A3, Canada*

[b] *Fuel Cell Research Laboratory (FCReL), School of Mechatronic Systems Engineering, Simon Fraser University, 250-13450 102 Avenue, Surrey, BC, V3T 0A3, Canada*

ARTICLE INFO

Article history:
Received 3 February 2015
Received in revised form
13 May 2015
Accepted 14 June 2015
Available online 6 July 2015

Keywords:
Micro porous layer
Effective diffusivity
PEM fuel cell
Analytical model
Unit cell

ABSTRACT

Gas diffusion layer, GDL, properties are crucial in determining the polymer electrolyte membrane fuel cell performance. The micro-porous layer, as a thin layer coated on the GDL that has a smaller pore size than the fibrous substrate, creates a considerable mass transport barrier to the incoming gases from the flow channels. Hence, the effective diffusivity of MPL can affect the overall performance of PEM fuel cell. In the present investigation, a new analytical model is developed, based on the unit cell approach, to find the effective diffusivity of the MPL. A compact relationship is proposed that can be used to estimate the effective MPL diffusivity as a function the MPL pore size distribution and porosity. The developed model is also used to find the sensitivity of the aforementioned design parameters on the effective diffusivity. It is found that the MPL pore size is as influential as the porosity on the effective diffusivity.

Introduction

The membrane electrode assembly (MEA) used in polymer electrolyte fuel cells consists of a membrane, two electrodes (anode and cathode), and two gas diffusion layers (GDLs). The GDL is responsible for providing the pathways for transport of the reactant gases from the flow channels to the catalyst layers. Hence, the mass transport resistance of this layer should be minimized for high performance operation. The GDL is typically a dual-layer carbon-based material composed of a macro-porous substrate, which usually contains carbon fibers, binder, and PTFE, and a thin delicate micro-porous layer (MPL), which is usually made of carbon nano-particles and PTFE. Usually spherical carbon nano-particles of 20–100 nm in diameter construct the complex structure of the MPL. Small pore sizes and highly hydrophobic characteristics are the two main specifications of the MPL.

Several reasons are behind the application of MPL inside the MEA. The main incentive for using this vulnerable layer is the enhancements achieved in fuel cell performance due to its assistance in the liquid water management [1,2]. This is

* *Corresponding author*. Tel.: +1 778 782 8538; fax: +1 778 782 1514.
E-mail addresses: mandishe@sfu.ca (M. Andisheh-Tadbir), melhanna@sfu.ca (M. El Hannach), ekjeang@sfu.ca (E. Kjeang), mbahrami@sfu.ca (M. Bahrami).

http://dx.doi.org/10.1016/j.ijhydene.2015.06.067

mainly a result of the small pore sizes and hydrophobic nature of the MPL that acts as an obstacle for penetration of liquid water into the fibrous substrate. Therefore, it forces the water to diffuse into the membrane, which helps the membrane hydration and reduces the ohmic losses in the membrane. Further, it reduces the chances of flooding in the GDL by transferring the liquid water from the cathode side towards the anode side through the electrolyte membrane. MPL also enhances the overall thermal/electrical conductivity of the MEA by reducing the contact resistances between the fibrous substrate and catalyst layer [2]; however, there are some other experimental evidences that show the MPL increases the overall thermal resistance by introducing a new layer [3].

Wide application of the MPL in the recent MEAs, rises the need for accurate models for estimating its transport properties. The effective diffusivity of the MPL is a key property in determining the fuel cell performance. However, since the MPL is a recently developed material, the number of published works with the focus on this thin and delicate layer is limited [4–14]. The number of publications are even less if one is looking for the effective transport properties, i.e., thermal/electrical conductivity, diffusivity [3,15–18]. Measuring the MPL diffusivity is a challenging task since the MPL needs a physical support and cannot be analyzed as a separate layer [16]. Similar to its measurements, modeling the MPL diffusivity is a difficult task [15,19], since it involves the reconstruction of the complex structure numerically and solving the diffusion equation in the nano-scale pores where the continuum assumption may be invalid and the Knudsen diffusion may prevail. Usually, complex numerical algorithms are employed to reconstruct a small portion of the MPL. This step is followed by a computationally intensive stage to solve the diffusion equations inside the void spaces of the reconstructed domain [15]. Although this approach leads to reliable and accurate results, an analytical relationship that correlates certain design parameters to the MPL diffusivity could be helpful and requires much less computational efforts.

Present relationships are either based on the effective medium theory [20,21], pore network models [22], percolation theories [23], or stochastic-based numerical modeling [24]. However, none of the existing methods are capable of providing an accurate, generally applicable function for the MPL diffusivity. Unit cell approach is another way of modeling the transport properties of porous materials. A unit cell is a simple geometry that inherits the most important specifications of a porous medium and roughly represents the entire medium structure. This approach is previously used by our colleagues in Refs. [3,25] to model the thermal conductivity of GDL and it is proven to be well applicable to model the transport properties of the fuel cell components. Hence, in this investigation an analytical modeling is performed based on the unit cell approach.

The main objective of this work is to propose a relationship for calculating the effective diffusivity of MPL. Hence, the heat and mass transfer analogy is utilized to find the effective diffusivity for a unit cell, which represents an MPL. The proposed relationship is suitable for implementation in complex performance models that require an accurate estimation of the effective transport properties.

Mathematical model

Unit cell geometry

A fully analytical solution of the mass transport equation inside a randomly structured porous material is not feasible. Simplifying assumptions are therefore required to derive an analytical model for predicting the transport properties of porous structures. In this work, the unit cell approach is used for modeling the effective diffusivity of MPL. Scanning electron microscopy, SEM, images from the surface and cross section of MPL helped us selecting a simplified geometry that represents the MPL structure. Fig. 1 shows an SEM image from the cross section of a typical MPL [13]. The structure of the MPL is complex and random; however, it is possible to divide structure into two domains: domain I that constitutes of large pores and domain II that is the packed bed of agglomerates surrounding those large pores. In Fig. 1 circles show the large pores (domain I) and their surrounding squares represent the packed bed of agglomerates (domain II).

In this investigation, a unit cell is devised that has both of these domains. The considered unit cell, which is shown in Fig. 2, is a cube that has a spherical pore with diameter d_I in the middle. The sphere is domain I, and its surrounding region in domain II, which is a homogeneous porous zone with the porosity of ε_{II} and the pore size of d_{II}. The relationship between the overall MPL porosity and the unit cell dimensions is found from the geometrical interrelations.

$$\varepsilon_{MPL} = \frac{V_{void}}{V_{tot}} = 1 - (1 - \varepsilon_{II})\left[1 - \frac{\pi d_I^3}{6a^3}\right] \quad (1)$$

In Eq. (1), the secondary domain's porosity, ε_{II}, primary pore diameter, d_I, and unit cell length, a, are unknown. Once the pore size distribution is known, these parameters can be calculated through a procedure that will be explained in the following paragraphs.

The average pore size for a porous zone can be found based on the probability density function of its pores. Hence, the average MPL pore size in this work is obtained from the following relationship.

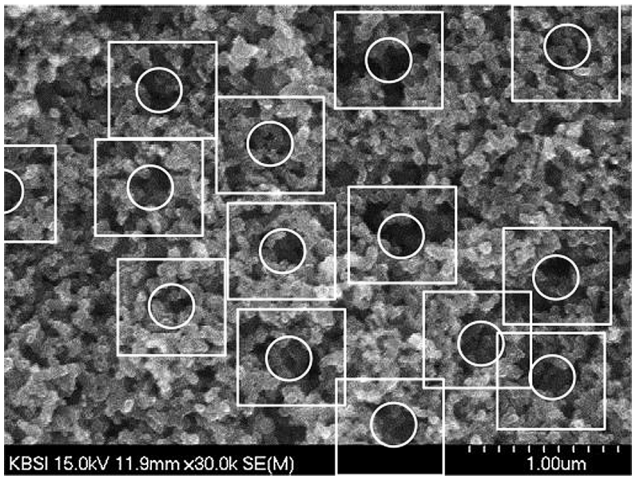

Fig. 1 – An SEM image from a cross section of an MPL [13].

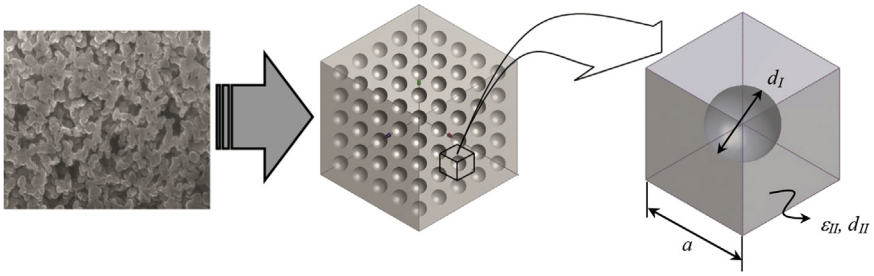

Fig. 2 – Considered unit cell in the present work.

$$d_{avg} = \sum_j f d_j = \sum_j \frac{V^j_{inc}}{V_{tot}} d_j \tag{2}$$

In Eq. (2), f is the probability of having a pore with diameter d_j, which is the ratio of the incremental pore size (V^j_{inc}) to the total volume of the pores V_{tot}. The information regarding the incremental and total pore volumes is obtained from the porosimetry measurements, e.g., by mercury intrusion porosimetry.

To associate the physical structure to the present model, d_I and d_{II} are needed to be defined and determined from the pore size distribution. The primary domain diameter, d_I, is defined as the average size for the pores that are larger than d_{avg}, in a similar fashion the secondary pore diameter, d_{II}, is the average size of the pores that are smaller than d_{avg}. Therefore, the three characteristic lengths,d_{avg}, d_I, and d_{II} are found respectively from the total average pore size, upper side average pore size, and lower side average pore size. As an instance, the pore size distribution of the MPL studied in Ref. [15] is shown in Fig. 3. Indicated in Fig. 3 are the average, primary, and secondary pore sizes, i.e., 125, 191, and 76 nm.

Note that in this work an MPL is modeled by a unit cell that has only two distinct pore sizes. So the pore size distribution for the considered unit cell has only two values d_I and d_{II}. Substituting these two pore sizes in Eq. (2) leads to a relationship between the pore size and other model parameters.

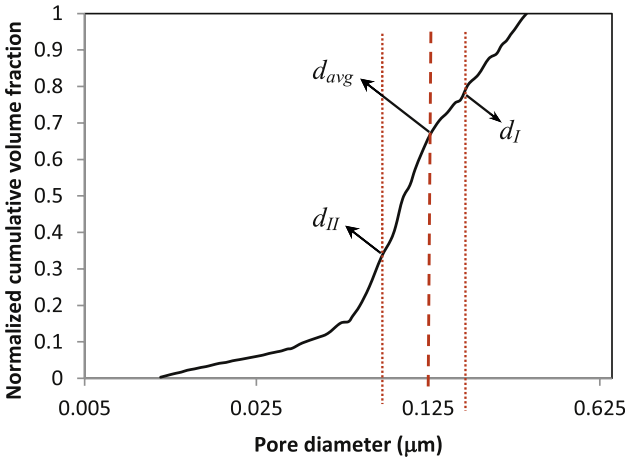

Fig. 3 – Pore size distribution of the MPL used in Ref. [15].

$$d_{avg} = \frac{V^I_{inc}}{V_{tot}} d_I + \frac{V^{II}_{inc}}{V_{tot}} d_{II} = \frac{\frac{\pi}{6} d_I^4 + \varepsilon_{II}\left(a^3 - \frac{\pi}{6} d_I^3\right) d_{II}}{\frac{\pi}{6} d_I^3 + \varepsilon_{II}\left(a^3 - \frac{\pi}{6} d_I^3\right)} \tag{3}$$

Simultaneous solution of Eqs. (1) and (3) gives the unit cell dimension, a, and the secondary zone porosity, ε_{II}. The porosity of the secondary zone, which is an effective porous medium around the primary domain, should be always smaller than or equal to the MPL porosity.

$$\varepsilon_{II} = \frac{(d_I - d_{avg})\varepsilon_{MPL}}{(d_{II} - d_{avg})\varepsilon_{MPL} + (d_I - d_{II})} \tag{4}$$

$$a = d_I \left(\frac{\pi}{6\left(1 - \frac{(1-\varepsilon_{MPL})}{1-\varepsilon_{II}}\right)} \right)^{\frac{1}{3}} \tag{5}$$

Heat and mass transfer analogy

After finding all the required geometrical parameters from the previous steps, in this section the details of the diffusivity model is explained. The effective diffusion coefficient can be calculated by using the analogy between the heat and mass transfer. The governing equation for the diffusion of heat or mass is the Laplace's equation with a diffusion coefficient, which is thermal conductivity for the transport of heat and mass diffusion coefficient for the transport of mass. Hence, using the heat conduction solution and replacing thermal conductivity with diffusivity, one can find the solution for the mass diffusion for the same geometry and similar boundary conditions. The effective thermal conductivity of a solid sphere embedded inside a cube is obtained analytically in Ref. [26] and is shown in Eq. (6).

$$k_{eff} = \frac{3k_c k_s \alpha + (2k_c + k_s)k_c(1-\alpha)}{3k_c \alpha + (2k_c + k_s)(1-\alpha)} \tag{6}$$

In Eq. (6) k_s and k_c are the thermal conductivities of sphere and cube, and α is the volume fraction of the sphere in the entire medium and is calculated as follows.

$$\alpha = \frac{\pi}{6}\left(\frac{d_I}{a}\right)^3 \tag{7}$$

Replacing the thermal conductivities with the diffusion coefficients of domains I and II, provide us with the desired relationship for the effective diffusivity of the unit cell.

$$D^{i}_{eff} = \frac{3D^{i}_{II}D^{i}_{I}\alpha\left(2D^{i}_{II} + D^{i}_{I}\right)D^{i}_{II}(1-\alpha)}{3D^{i}_{II}\alpha + \left(2D^{i}_{II} + D^{i}_{I}\right)(1-\alpha)} \quad (8)$$

where D^{i}_{eff} is the effective diffusivity of species i through the MPL, D^{i}_{I} is the gas diffusion coefficient in domain I (the spherical pore), and D^{i}_{II} is the gas effective diffusion coefficients of the ith species in domain II (the effective porous medium around the domain I).

To calculate the gas diffusion coefficient in domain I and II, the diffusion regime needs to be determined. Diffusion mainly occurs due to collision of gas molecules to each other and to the pore walls. The former is called bulk diffusion and the latter is called Knudsen diffusion. To determine the appropriate diffusion mechanism in a medium, Knudsen number is calculated through Eq. (9).

$$Kn = \frac{\lambda}{l} \quad (9)$$

In Eq. (9), λ is the mean free path of gas molecules and l is the characteristic length scale of the medium. When Kn << 1, we are in continuum regime and the diffusion process is dominated by the bulk diffusion. Conversely, when Kn >> 1 the diffusion process is dominated by the Knudsen diffusion. In the MPL, the pore sizes are in the range of 20–300 nm. Considering the mean free path of 63 nm for oxygen at standard conditions [27], Knudsen number is found to be ~0.2–3.0. This implies that the transport of species inside the MPL is occurring in the mixed diffusion regime, where both Knudsen and bulk diffusion are contributing to the diffusion phenomenon.

Equation (10) shows the Bosanquet's formula [28], which is used in this work to calculate the diffusion coefficient in the mixed diffusion regime.

$$D_i = \left[\frac{1}{D^{b}_{i}} + \frac{1}{D^{Kn}_{i}}\right]^{-1} \quad (10)$$

Bulk diffusion coefficients for different species can be found in the open literature as functions of pressure and temperature. For instance, bulk diffusion coefficient for an oxygen–nitrogen pair at different pressures and temperatures can be found from Eq. (11) [29],

$$\ln\left(pD^{b}_{O_2}\right) = \ln(1.13\times10^{-5}) + 1.724\ln T \quad (11)$$

where p is the pressure in [atm], T is the gas temperature in [K], and $D^{b}_{O_2}$ is the bulk diffusion coefficient of oxygen in [$cm^2\ s^{-1}$].

To obtain the Knudsen diffusion, Eq. (12) is used [30], in which d is a characteristic length scale of the medium, R is the universal gas constant, and M_i is the molecular mass of the ith species.

$$D^{Kn}_{i} = \frac{4}{3}d\sqrt{\frac{RT}{2\pi M_i}} \quad (12)$$

D_I, which is the gas diffusion coefficient of the stored gas inside the primary pore, can be obtained by substituting Eq. (13) in (9) with d_I as the pore size. Therefore, D_I can be found from the following.

$$D^{i}_{I} = \left(\frac{1}{D^{i}_{b}} + \frac{3}{d_I}\sqrt{\frac{\pi M_i}{8RT}}\right)^{-1} \quad (13)$$

The effective gas diffusion coefficient in domain II, D_{II}, needs to be calculated from the available relationships for the effective diffusivity for packed beds. Several equations are available in the literature for estimating the effective diffusivity inside a porous material. Some of the most common ones are listed in Table 1. In Table 1, D is the diffusion coefficient of the gas inside the pores and D_{eff} is the effective diffusion coefficient in the porous medium. Therefore, for a medium with large pore size, where Kn << 1, D is the bulk diffusion; for a medium with Kn ~ 1, D should be calculated through Eq. (9); and for a medium with very small pore size, where Kn >> 1, D should be obtained from Eq. (11). In this work to estimate the effective diffusivity in domain II, the formula proposed by Mezedure et al. [22] is utilized. This formula is obtained for various size spherical particles and as it is discussed later in this paper, it gives the closest values to the published data in the literature.

Fig. 4 presents the predicted effective diffusivities, by the models introduced in Table 1, for seven different MPL structure reported in literature. Comparing the predicted diffusivities with the available data in the literature, a considerable difference is observed. Bruggeman's approximation [20], Neale and Nader relationship [21], and Tomadakis and Sotirchos' formula [23] over predict the data considerably, while Zamel et al.'s model [24] under predict the actual values. The closest model to the published data is Mezedur et al.'s formula [22]. Therefore, this model is implemented in the present investigation to approximate the effective diffusivity of in domain II. Note that Mezedur et al.'s model fails to capture the trends of data in some cases, that is why it needs to be modified to be used for MPL.

To get D_{II}, Mezedur et al.'s formula is used [22]; however, D is substituted by the modified diffusion coefficient for a pore of diameter d_{II}. The following is the obtained relationship for calculating D_{II}.

$$D^{i}_{II} = \left[1-(1-\varepsilon_{II})^{0.46}\right]\left(\frac{1}{D^{i}_{b}} + \frac{3}{d_{II}}\sqrt{\frac{\pi M_i}{8RT}}\right)^{-1} \quad (14)$$

The sequence of calculations to obtain the effective MPL diffusivity is depicted in Fig. 5.

Results and discussion

In this section, first, the results from the present work are compared with the available data in the literature. Then, the effects of MPL pore size and porosity on the effective diffusivity are examined.

Model validation

There are only a few experimental data points available for the MPL diffusivity in the literature [15,16]. In a research conducted in our team, the MPL diffusivity is obtained by using the FIB/SEM technique [15]. In that work, the relative diffusivity for their considered MPL was obtained 0.15 ± 0.03

Table 1 – Available relations for the effective diffusivity of a porous medium.

Reference	Relationship	Note
Bruggeman [20]	$D_{eff} = D\varepsilon^{1.5}$	Packed spherical particles
Mezedur et al. [22]	$D_{eff} = D[1-(1-\varepsilon)^{0.46}]$	Multi length scale particle based porous media
Tomadakis and Sotirchos [23]	$D_{eff} = D\varepsilon(\varepsilon - 0.11/1 - 0.11)^{0.785}$	Fibrous porous media
Neale and Nader [21]	$D_{eff} = D(2\varepsilon/3-\varepsilon)$	Packed spherical particles
Zamel et al. [31]	$D_{eff} = D(1-2.76\varepsilon\cosh(3\varepsilon-1.92)[3(1-\varepsilon)/3-\varepsilon])$	Fibrous gas diffusion layers

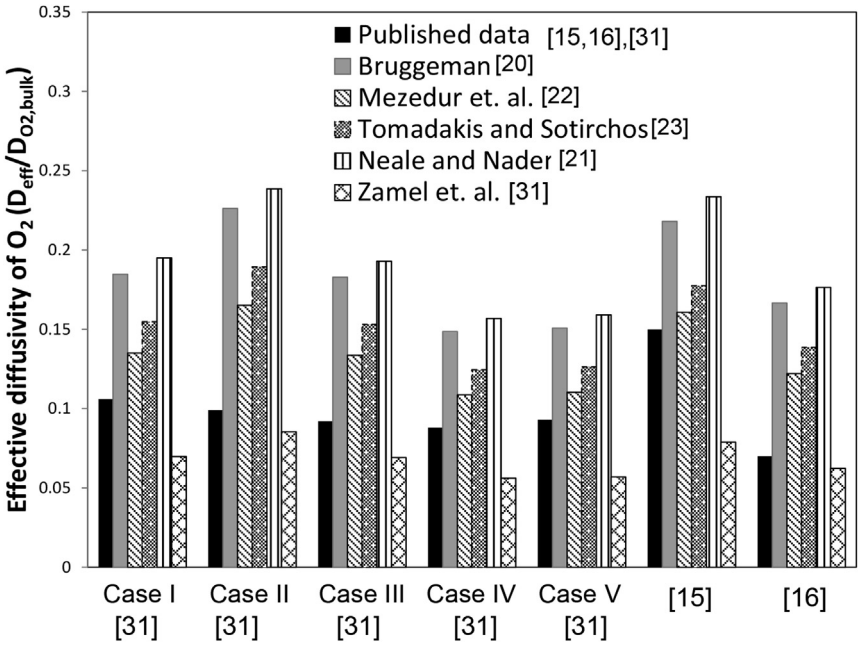

Fig. 4 – Comparison of the available diffusivity models in the literature to published data [15,16], and [31].

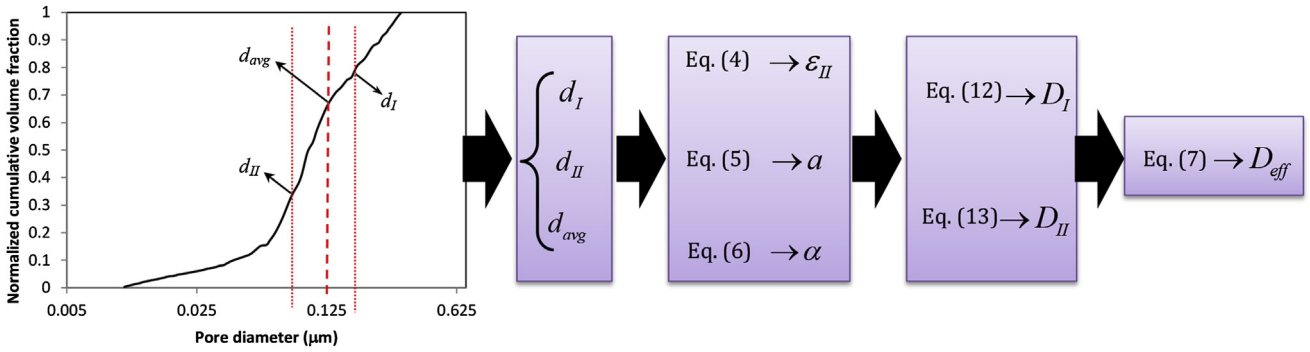

Fig. 5 – Steps for calculating the effective diffusivity using the proposed model.

for oxygen. The porosity of the MPL was reported as 62%. To use the present model, the values for d_{avg}, d_I and d_{II} needs to calculated from the pore size distribution, *c.f.* Fig. 3. Following the approach presented in section Unit cell geometry, the respective values for d_{avg}, d_I and d_{II} are obtained as 124, 191, and 76 nm. Substituting these values into the present model, *cf.* Fig. 5, the relative diffusivity is calculated as 0.157 for oxygen, which deviates from the measured data by less than 5%.

Chan et al. [16] also did another measurement on the GDL diffusivity (fibrous substrate and MPL) using a Loschmidt cell. Their reported value for the effective oxygen diffusivity inside the MPL was $1.5 \pm 0.2 \times 10^{-6}$ m^2 s^{-1}, which was equal to the relative diffusivity of0.07 ± 0.01. Their MPL porosity was 64% and the primary and secondary pores extracted from the reported pore size distribution were 204 and 44 nm, respectively. Inserting these parameters into the present model leads to 0.068 for the relative diffusivity of oxygen, i.e., less than 3% deviation.

In another work, Zamel et al. [31] reported the effective diffusivity for five different MPLs that were constructed

Table 2 – Description of the cases investigated in Ref. [31] [a].

Case	Porosity (%)	d_{avg} (nm)	d_I (nm)	d_{II} (nm)
I	65	66	87	45
II	65	92	124	36
III	65	65	116	38
IV	65	48	99	30
V	65	49	71	31

[a] The present pore sizes are extracted from the reported pore size distributions in Ref. [31].

through stochastic numerical model. These cases are introduced in Table 2. The predicted values for these MPLs by the present model are shown in Fig. 6 and are compared to the published data. The estimated values by Mezedur et al. [22]. approach is also shown in Fig. 6 that reveal this model overpredicts the effective diffusivity for most cases. Specially, for case II, where the pore size distribution has two peaks, because in the present model, the entire structure is modeled with two distinct pores, which would be close to the two peaks in case of MPLs with bimodal pore size distribution. The present model shows a reasonable accuracy with maximum deviation of around 15%.

Effect of liquid water

In this model, the effect of liquid water inside the MPL is not considered. Because it is expected that the volume fraction of liquid water inside the MPL is low due to the high hydrophobicity of the MPL and its small pore sizes. These two characteristics of the MPL impede liquid water entering to the MPL and push it towards the membrane. Therefore, water is transferred from the MPL to the GDL and cathode flow channels mostly in the form of water vapor. In case of high saturation levels inside the MPL, some modifications to the model should be made, e.g., multiplying a $(1-s)^m$ term to the results [32], where s is the saturation level. The accurate way of extending the model to predict the diffusivity values, when liquid water is present, is to know the liquid water distribution in the structure and treat the liquid water droplets as solid phase. This means the liquid water blocks the pathways for gas diffusion.

Parametric study

In this section, a parametric study is performed to investigate the effects of various parameters on the effective diffusivity of MPL, using the proposed model. The input parameters to model are the pore size distribution and MPL porosity. Although manufacturing some of the assumed structures in this section may not be feasible, the parametric study performed here will provide the GDL manufacturers with useful information, especially the trends in diffusivity of MPL as a function of structural parameters.

MPL pore size distribution

The MPL pore size distribution is a controlling parameter in determining its effective diffusivity. The pore sizes in the MPL can be controlled using different pore forming agents and different drying conditions [13]. Furthermore, as discussed in Refs. [33] and [34], the MPL porosity and pore size distribution alter with different PTFE contents. In this section, the effective diffusivities for some arbitrarily chosen MPL pore size distributions are obtained. It is tried to cover a wide range of possible pore size distributions. These cases are named based on their corresponding diameters; namely d_{II}, d_{avg}, and d_I values. The porosity of the MPLs is considered 60% for these five cases. Note that although the effect of PTFE content on

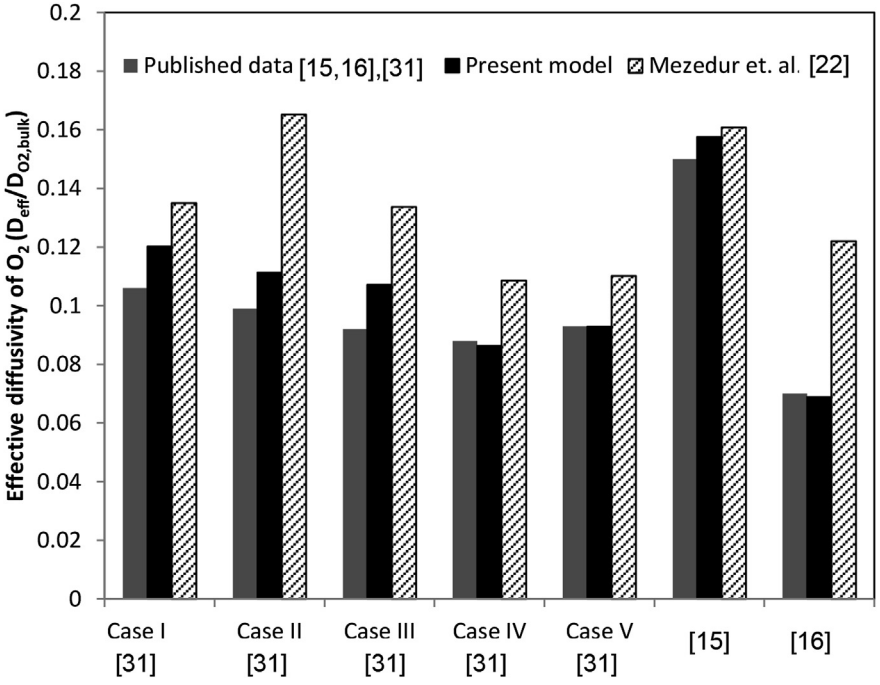

Fig. 6 – Comparison of the model results with other diffusivity values from the literature.

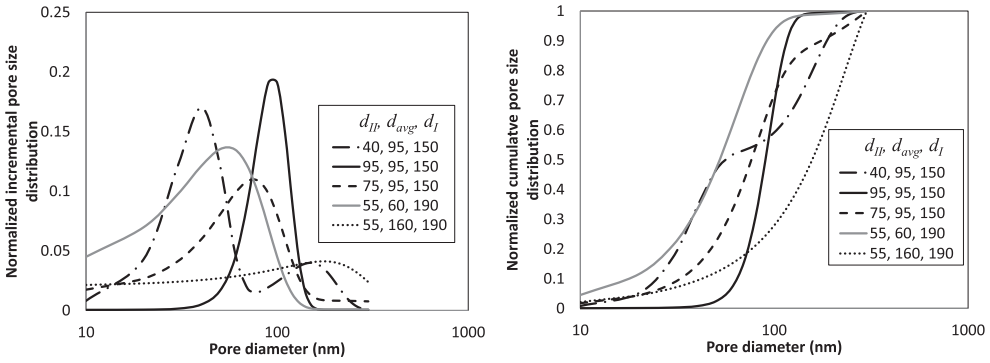

Fig. 7 – The incremental (a), and the cumulative (b), pore size distributions for the five cases studied in section MPL pore size distribution.

diffusivity is not included in the present model explicitly, the obtained pore size distribution from mercury intrusion porosimetry, implicitly includes those effects.

Fig. 7 shows the pore size distributions of the MPLs for which the effective diffusivity values are calculated. To generate these distributions, it is assumed the pores are distributed normally. Hence, the normal probability density function, *c.f.* Eq. (15), is used.

$$f(x) = \frac{\exp\left(-\frac{1}{2}\left(\frac{x-\mu}{\sigma}\right)^2\right)}{\sigma\sqrt{2\pi}} \tag{15}$$

In Eq. (15), μ and σ are the mean and variance of the pore sizes. To find a pore size distribution for a specific MPL with specific values of d_I, d_{II}, and d_{avg}, the normal probability density functions with the mean values of d_I and d_{II} should be first summed up. Then the variance of each distribution should be changed until the mean value of the summation of these two distributions becomes equal to the desired average pore diameter. Note that various pore size distributions might exist for a certain d_I, d_{II}, and d_{avg}.

For the first three cases, the average and primary pore diameters are considered 95 and 150 nm respectively, and the secondary pore diameter is varied. In the last two cases, the average pore diameter is altered. The effective diffusivity of oxygen for each of these cases is plotted in Fig. 8. Comparing the first three cases, it is observed that by increasing the secondary pore size, the effective diffusivity increases significantly. If the total volume of smaller pores in the pore size distribution of an MPL is large and the peak of the incremental pore size distribution shifts towards the left, a small effective diffusivity should be expected.

For the last two cases where only the average pore size is varied, no considerable change is observed in the calculated effective diffusivity. However, by looking at variations of the effective diffusivity at different average pore size in Fig. 9, an optimum pore size is found at which the effective diffusivity is a maximum. For the three porosities plotted in Fig. 9, the optimum value of the average pore size and MPL porosity can be found from the following correlation. Note that this equation is obtained for $55\% < \varepsilon_{MPL} < 65\%$ and may not be applicable to larger/smaller porosity values.

$$d_{avg}^{opt} = 2.166\varepsilon_{MPL} \tag{16}$$

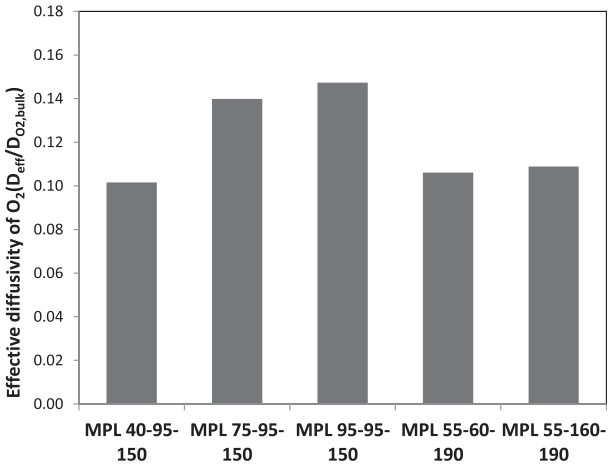

Fig. 8 – Effective diffusivity of the MPLs introduced in Fig. 7.

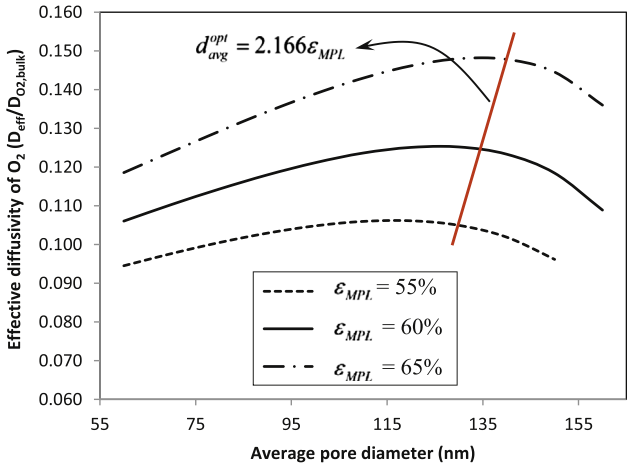

Fig. 9 – Variations of the effective diffusivity at different average pore size.

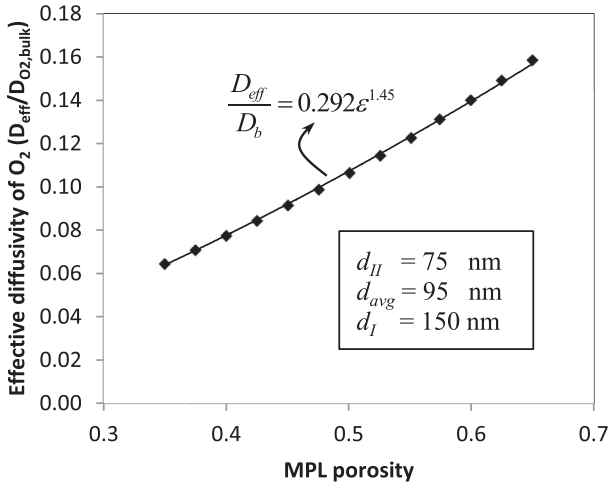

Fig. 10 – Variations of effective oxygen diffusivity by MPL porosity.

In Eq. (16), the unit for the optimum average pore diameter d_{avg}^{opt}, is [nm], and the MPL porosity is considered in percent.

MPL porosity

Plotted in Fig. 10 is the MPL diffusivity as a function of its porosity. Here, the pore size distribution is considered fixed and the MPL porosity is varied between 35% and 65%. There is a 145% increase in the effective diffusivity when the MPL porosity is increased in this range. At lower porosities, mass transfer resistance is higher because the material is denser. So that the pathways for gas transport are narrower. This increases the contribution of Knudsen diffusion in the overall mass transfer process, and consequently reduces the effective diffusivity.

For the specified pore size distribution, the data can be fitted by $D_{eff}/D_b = 0.292\varepsilon^{1.45}$, which as an instance, is different from what Bruggeman's model [20] can predict, i.e., $D_{eff}/D_b = \varepsilon^{1.5}$. Here, only the Bruggeman's model is used for comparison, since it is simpler than other models and it is shown previously in other works that it over-predicts the properties [31]. Other models will also fail in predicting the MPL diffusivity for the same reasons explained in section Heat and mass transfer analogy.

Conclusion

In this study, a unit cell approach was used to model the effective diffusivity of MPLs analytically. A unique geometrical model was developed as the unit cell for the MPL. The available SEM images of the MPL were used to devise an appropriate unit cell for modeling. The unit cell was consisting of a spherical pore inside a porous cube. The analogy between the heat and mass transfer was utilized to find the effective diffusivity coefficient for the unit cell. The obtained results from the proposed analytical relationship were compared to the experimental and numerical data available in the literature. Agreement between the present model's results and the available data were promising. The model was then used to find the sensitivity of the effective diffusivity to some of the structural parameters of the MPL. It was found that both the pore size distribution and porosity were influential in determining the effective MPL diffusivity.

In summary, the findings of this research can be listed as the followings:

- A new compact relationship was proposed to predict the effective MPL diffusivity as a function of the pore size distribution and porosity of the MPL.
- Effects of PTFE content on diffusivity was not studied directly, but the changes in pore size distribution and porosity due to addition of PTFE and their effects on diffusivity could be studied using the proposed model.
- Pore size was as influential on the effective diffusivity as the porosity. However, it is not easy to choose one as the main influential property. Since they are both effective on the final diffusivity value to the same extent and effects of both of them should be considered.
- Increasing porosity and the secondary domain pore size, d_{II}, would increase the effective diffusivity.

Acknowledgments

The authors gratefully acknowledge the financial support from the Natural Sciences and Engineering Research Council of Canada.

Nomenclature

a	unit cell dimension, m
d	diameter, m
D	diffusion coefficient, $m^2\ s^{-1}$
k	thermal conductivity $W\ m^{-1}\ K^{-1}$
l	length scale, m
M	molecular mass, $kg\ mol^{-1}$
p	pressure, atm
R	universal gas constant, $8.314\ J\ K^{-1}\ mol^{-1}$
T	temperature, K
V	volume, m^3

Greek symbols

α	volume fraction of sphere in the medium, Eq. (6)
ε	porosity
λ	mean free path, m

Subscripts

I	primary
II	secondary
tot	total
avg	average
inc	incremental
eff	effective
s	sphere
c	cube
b	bulk

REFERENCES

[1] Pasaogullari U, Wang CY, Chen KS. J Electrochem Soc 2005;152:A1574.
[2] Weber AZ, Newman J. J Electrochem Soc 2005;152:A677.
[3] Sadeghifar H, Djilali N, Bahrami M. J Power Sources 2014;248:632.
[4] Yan WM, Wu DK, Wang XD, Ong AL, Lee DJ, Su A. J Power Sources 2010;195:5731.
[5] Spernjak D, Fairweather J, Mukundan R, Rockward T, Borup RL. J Power Sources 2012;214:386.
[6] Chun JH, Park KT, Jo DH, Kim SG, Kim SH. Int J Hydrogen Energy 2011;36:1837.
[7] Schweiss R, Steeb M, Wilde PM, Schubert T. J Power Sources 2012;220:79.
[8] Kitahara T, Konomi T, Nakajima H. J Power Sources 2010;195:2202.
[9] Gallo Stampino P, Cristiani C, Dotelli G, Omati L, Zampori L, Pelosato R, et al. Catal Today 2009;147:S30.
[10] Tang H, Wang S, Pan M, Yuan R. J Power Sources 2007;166:41.
[11] Wang XL, Zhang HM, Zhang JL, Xu HF, Tian ZQ, Chen J, et al. Electrochim Acta 2006;51:4909.
[12] Chun JH, Park KT, Jo DH, Lee JY, Kim SG, Park SH, et al. Int J Hydrogen Energy 2011;36:8422.
[13] Chun JH, Park KT, Jo DH, Lee JY, Kim SG, Lee ES, et al. Int J Hydrogen Energy 2010;35:11148.
[14] Wargo E a, Schulz VP, Çeçen a, Kalidindi SR, Kumbur EC. Electrochim Acta 2013;87:201.
[15] Nanjundappa A, Alavijeh AS, El Hannach M, Harvey D, Kjeang E. Electrochim Acta 2013;110:349.
[16] Chan C, Zamel N, Li X, Shen J. Electrochim Acta 2012;65:13.
[17] Burheim OS, Su H, Pasupathi S, Pharoah JG, Pollet BG. Int J Hydrogen Energy 2013;38:8437.
[18] Pant LM, Mitra SK, Secanell M. J Power Sources 2012;206:153.
[19] Ostadi H, Rama P, Liu Y, Chen R, Zhang XX, Jiang K. J Memb Sci 2010;351:69.
[20] Bruggeman DAG. Ann Der Phys 1935;24:636.
[21] Neale GH, Nader WK. AIChE J 1973;19:112.
[22] Mezedur MM, Kaviany M, Moore W. AIChE J 2002;48:15.
[23] Tomadakis MM, Sotirchos SV. AIChE J 1993;39:397.
[24] Zamel N, Li X, Shen J. Energy Fuels 2009;23:6070.
[25] Sadeghifar H, Bahrami M, Djilali N. J Power Sources 2013;233:369.
[26] Carslaw HS, Jaeger JC. Conduction of heat in solids. 2nd ed. London: Oxford University Press; 1959.
[27] Hirschfelder JO, Curtiss RB. Molecular theory of gases and liquids. New York: John Wiley; 1954.
[28] Pollard WG, Present RD. Phys Rev 1948;73:762.
[29] Marrero TR, Mason EA. J Phys Chem Ref Data 1972;1:3.
[30] Kast W, Hohenthanner CR. Int J Heat Mass Transf 2000;43:807.
[31] Zamel N, Becker J, Wiegmann A. J Power Sources 2012;207:70.
[32] Nam JH, Kaviany M. Int J Heat Mass Transf 2003;46:4595.
[33] Park S, Lee JW, Popov BN. J Power Sources 2008;177:457.
[34] Tseng CJ, Lo SK. Energy Convers Manag 2010;51:677.